nature cell biology

ARTICLES

Auxin regulates aquaporin function to facilitate lateral root emergence

Benjamin Péret[1,6,7], Guowei Li[2,7], Jin Zhao[3,7], Leah R. Band[1,7], Ute Voß[1], Olivier Postaire[2], Doan-Trung Luu[2,6], Olivier Da Ines[3,6], Ilda Casimiro[4], Mikaël Lucas[1], Darren M. Wells[1], Laure Lazzerini[1], Philippe Nacry[2], John R. King[1], Oliver E. Jensen[1,5], Anton R. Schäffner[3,8], Christophe Maurel[2,8] and Malcolm J. Bennett[1,8]

Aquaporins are membrane channels that facilitate water movement across cell membranes. In plants, aquaporins contribute to water relations. Here, we establish a new link between aquaporin-dependent tissue hydraulics and auxin-regulated root development in *Arabidopsis thaliana*. We report that most aquaporin genes are repressed during lateral root formation and by exogenous auxin treatment. Auxin reduces root hydraulic conductivity both at the cell and whole-organ levels. The highly expressed aquaporin PIP2;1 is progressively excluded from the site of the auxin response maximum in lateral root primordia (LRP) whilst being maintained at their base and underlying vascular tissues. Modelling predicts that the positive and negative perturbations of PIP2;1 expression alter water flow into LRP, thereby slowing lateral root emergence (LRE). Consistent with this mechanism, *pip2;1* mutants and *PIP2;1*-overexpressing lines exhibit delayed LRE. We conclude that auxin promotes LRE by regulating the spatial and temporal distribution of aquaporin-dependent root tissue water transport.

The establishment of a mature root system is achieved through repetitive branching of the primary root. This process—called lateral root formation—is initiated deep within the primary root from a small subset of pericycle cells[1]. The growth of a new LRP coincides with its emergence through the outer tissues[2]. The tight coordination of lateral root formation and emergence is controlled by auxin[3,4], which acts as a local inductive signal and favours cell separation in the overlaying tissues[5].

The biomechanics of LRP growth and its potential link with auxin are only partially understood[5]. In particular, the role of tissue water transport during LRE has not been examined. In addition to the formation of new cells, plant tissues grow when cell walls relax and extend in response to the cell's turgor pressure[6]. Sustained growth is primarily driven by solute uptake and maintenance of cell osmotic potential, and requires sufficient water inflow to keep turgor above yield threshold[7]. The water needed for growth is typically supplied either through the vasculature or the soil, before being transferred from cell to cell[7]. Therefore, the hydraulics of the whole plant or expanding tissues can be critical[8,9]. Although water transport is known to affect growth of leaves and primary roots[8,10], its significance during LRE has not been explored. Yet, the LRP is symplastically isolated from the primary root vasculature[11], suggesting the need for efficient transcellular water fluxes towards the dividing and expanding cells.

Aquaporins represent a large class of membrane channels present in most living organisms[12]. In plants, aquaporins fall into seven subfamilies[13], which include plasma membrane intrinsic proteins (PIPs) and the tonoplast intrinsic proteins (TIPs). Their role in plant water relations has been studied and linked to a wide range of functions[14,15], including root water uptake and regulation of tissue hydraulic conductance under environmental stresses.

To address the hydraulics of LRP growth and emergence, we studied the role of aquaporins during early stages of lateral root development

[1]Centre for Plant Integrative Biology, University of Nottingham, LE12 5RD, UK. [2]Biochimie et Physiologie Moléculaire des Plantes, Institut de Biologie Intégrative des Plantes, Unité Mixte de Recherche 5004 Centre National de la Recherche Scientifique - Unité Mixte de Recherche 0386 Institut National de la Recherche Agronomique - MontpellierSupAgro - Université Montpellier 2, 2 Place Viala, F-34060 Montpellier Cedex 2, France. [3]Institute of Biochemical Plant Pathology, Helmholtz Zentrum München, 85764 Neuherberg, Germany. [4]Universidad de Extremadura, Facultad de Ciencias, Badajoz 06006, Spain. [5]School of Mathematics, University of Manchester, M13 9PL, UK. [6]Present addresses: Unité Mixte de Recherche 7265 Commissariat à l'Energie Atomique et aux Energies Alternatives, Centre National de la Recherche Scientifique, Laboratoire de Biologie du Développement des Plantes, Université d'Aix-Marseille, 13108 Saint-Paul-lez-Durance, France (B.P.); Université des Sciences et Techniques de Hanoï, Institut de Recherche pour le Développement Laboratoire Mixte International Rice, Agronomical Genetics Institute, Ha Noi, Vietnam (D-T.L.); Génétique, Reproduction et Développement, Unité Mixte de Recherche 6293 Centre National de la Recherche Scientifique, Institut National de la Santé et de la Recherche Médicale U1103, Université de Clermont-Ferrand, Aubière 63170, France (O.D.I.). [7]These authors contributed equally to this work. [8] Correspondence should be addressed to A.R.S., C.M. or M.J.B. (e-mail: schaeffner@helmholtz-muenchen.de or maurel@supagro.inra.fr or malcolm.bennett@nottingham.ac.uk)

Received 28 June 2011; accepted 8 August 2012; published online 16 September 2012; DOI: 10.1038/ncb2573

in *Arabidopsis*. We observed that most aquaporin genes are repressed during lateral root formation in an auxin-dependent manner. As a result, auxin represses root cell hydraulic conductivity. We describe how auxin-related changes in aquaporin distribution may be important for organ emergence and provide converging mathematical and genetic evidence that aquaporins facilitate LRE. Our results demonstrate a complex spatial and temporal interaction between auxin and aquaporin function, to support LRP growth.

RESULTS

Most aquaporin genes are repressed by auxin during lateral root formation

We initially considered whether aquaporin expression was altered during lateral root development. Lateral root initiation can be induced by either mechanical[16,17] or gravitropic[18,19] stimuli. Following a 90° gravitropic stimulus, lateral roots develop in a highly synchronized manner at the outer edge of a bending root (Fig. 1a,b). Stage I primordia[20] were first detected 18 h post-gravitropic induction (pgi); then primordia for each subsequent stage were detected approximately every 3 h, until emergence at stage VIII, ~42 h pgi (Fig. 1b). We profiled aquaporin gene expression during lateral root development at high temporal resolution (that is, at every stage of lateral root development) by micro-dissecting root bends every 6 h pgi.

Profiling all 13 PIP and four highly expressed TIP isoforms by real-time quantitative PCR with reverse transcription (RT–qPCR) revealed that 14 of the 17 genes were repressed during lateral root development whereas *PIP1;4* and *PIP2;5* showed no or little induction (Fig. 1c,d). In contrast, *PIP2;8* was induced up to tenfold 36 h pgi (Fig. 1d). Repression of most aquaporin genes occurred during early lateral root formation (about 6 pgi), corresponding to when auxin accumulates in pericycle founder cells[21]. However, four *PIP* genes, including the highly expressed isoforms *PIP2;1* and *PIP2;2* (refs 22,23), showed a delayed repression at >10 h pgi (Fig. 1c).

Auxin is a key signal during early stages of lateral root development[4]. Treatment of whole roots with the auxin indole-3-acetic acid (IAA) induced an overall inhibition of aquaporin gene expression (Fig. 1e). Whereas *PIP1;3* and *PIP2;4* showed up to twofold induction, the 15 other *PIP* and *TIP* genes were repressed after IAA treatment (Fig. 1e,f). Only *PIP2;5* and *PIP2;8* recovered and even overshot their previous level. The similar expression profiles following gravity and auxin treatments suggest that auxin is responsible for the repression of aquaporin gene expression during LRE. The temporal differences observed are likely to reflect the synchronous and asynchronous cellular responses to endogenous and exogenous auxin sources, respectively. Nevertheless, our results reveal that auxin represses the expression of most aquaporin genes in the *Arabidopsis* root.

Auxin controls root aquaporin expression through ARF7

Auxin response factor (ARF) proteins function as transcription factors controlling auxin-responsive genes[24]. ARF7 plays a key role during lateral root formation and emergence[5,25–28]. Thus, we determined the effects of the *arf7* loss-of-function on *PIP* and *TIP* expression. For *PIP1;1*, *PIP1;4*, *PIP2;1*, *PIP2;2* and *PIP2;7* showing sustained auxin-dependent repression, a diminution of hormone effects was observed in the *arf7* mutant (Fig. 2a and Supplementary Fig. S1). Expression of the remaining auxin-repressed *PIP* genes was similar between the two backgrounds. Interestingly, auxin induction of *PIP1;3* and *PIP2;5* was also ARF7 dependent.

Next, we investigated whether transcriptional repression of aquaporin genes by auxin resulted in reduced aquaporin protein content. Enzyme-linked immunosorbent assays (ELISAs) using an antibody specific for PIP2;1, PIP2;2 and PIP2;3 (ref. 29) revealed a strong diminution of these aquaporins in the root, to 79% and 45%, at 18 and 42 h after auxin treatment, respectively (Fig. 2b). In contrast, the *arf7* mutation counteracted the auxin-induced reduction of these aquaporins (Fig. 2b). We conclude that auxin diminishes the accumulation of these aquaporins by inhibiting their expression in an ARF7-dependent manner.

Auxin controls root hydraulics and cell turgor through ARF7

To examine the effects of auxin on aquaporin function, roots of hydroponically grown plants were treated with IAA and their water-transport properties were characterized[30]. The root water permeability measured with a pressure chamber (hydrostatic hydraulic conductivity, $Lp_{r\text{-}h}$; ref. 30) was not affected on short auxin treatments (Supplementary Fig. S2a). However, longer treatments triggered a large drop in $Lp_{r\text{-}h}$ (by up to 69%; Fig. 2c). When measured under conditions of free sap exudation[30], root water permeability (osmotic hydraulic conductivity, $Lp_{r\text{-}o}$) also showed a marked (−51%) inhibition after 42 h of auxin treatment (Supplementary Fig. S2b). Interestingly, $Lp_{r\text{-}h}$ of *arf7* was insensitive to auxin inhibition (Fig. 2c). Yet, the *arf7* $Lp_{r\text{-}h}$ was inhibited by 5 mM H_2O_2 (Supplementary Fig. S2c). This aquaporin-blocking treatment[31] demonstrates that *arf7* specifically altered aquaporin inhibition by auxin. Hence, ARF7 plays a central role in auxin-dependent regulation of aquaporins in the *Arabidopsis* root.

To determine whether auxin-dependent regulation of aquaporin function also applies to root cortical cells, the water relation parameters of these cells were deduced using a cell pressure probe[30] (Supplementary Fig. S2d–f). A drop in cortical cell hydraulic conductivity (Lp_{cell}) by 48% was observed 18 h after IAA application (Fig. 2d). A longer (42 h) auxin treatment triggered a strong reduction of cortical cell turgor, in accordance with older reports in cucumber hypocotyls[32]. In contrast, the cortical cell turgor remained constant in the *arf7* mutant (Fig. 2e). Our data indicate a dual effect of auxin on cortical cell water relations, both of which are under the control of ARF7.

Auxin alters aquaporin spatial expression during lateral root development

Our expression and functional studies suggest that auxin-regulated aquaporin gene expression may play an important role during lateral root development. To investigate this further, we focused on PIP2;1, one of the most highly expressed aquaporins in roots[22,23] that was regulated by auxin in an ARF7-dependent manner. A loss-of-function mutant (*pip2;1-2*; ref. 33) showed a decrease by 14% ($p < 0.01$) in $Lp_{r\text{-}o}$, indicating that PIP2;1 contributes significantly to root hydraulics (Fig. 2f and Supplementary Fig. S2g–j).

Expression studies using transcriptional (*proPIP2;1:GUS*) and translational (*proPIP2;1:PIP2;1–mCHERRY*) fusions revealed that *PIP2;1* is highly expressed in the stele and less in outer root layers (Fig. 3a,d,e). *PIP2;1* is expressed in stage I LRP (Fig. 3a,d), but from stage III onwards *PIP2;1* expression is excluded from LRP tips

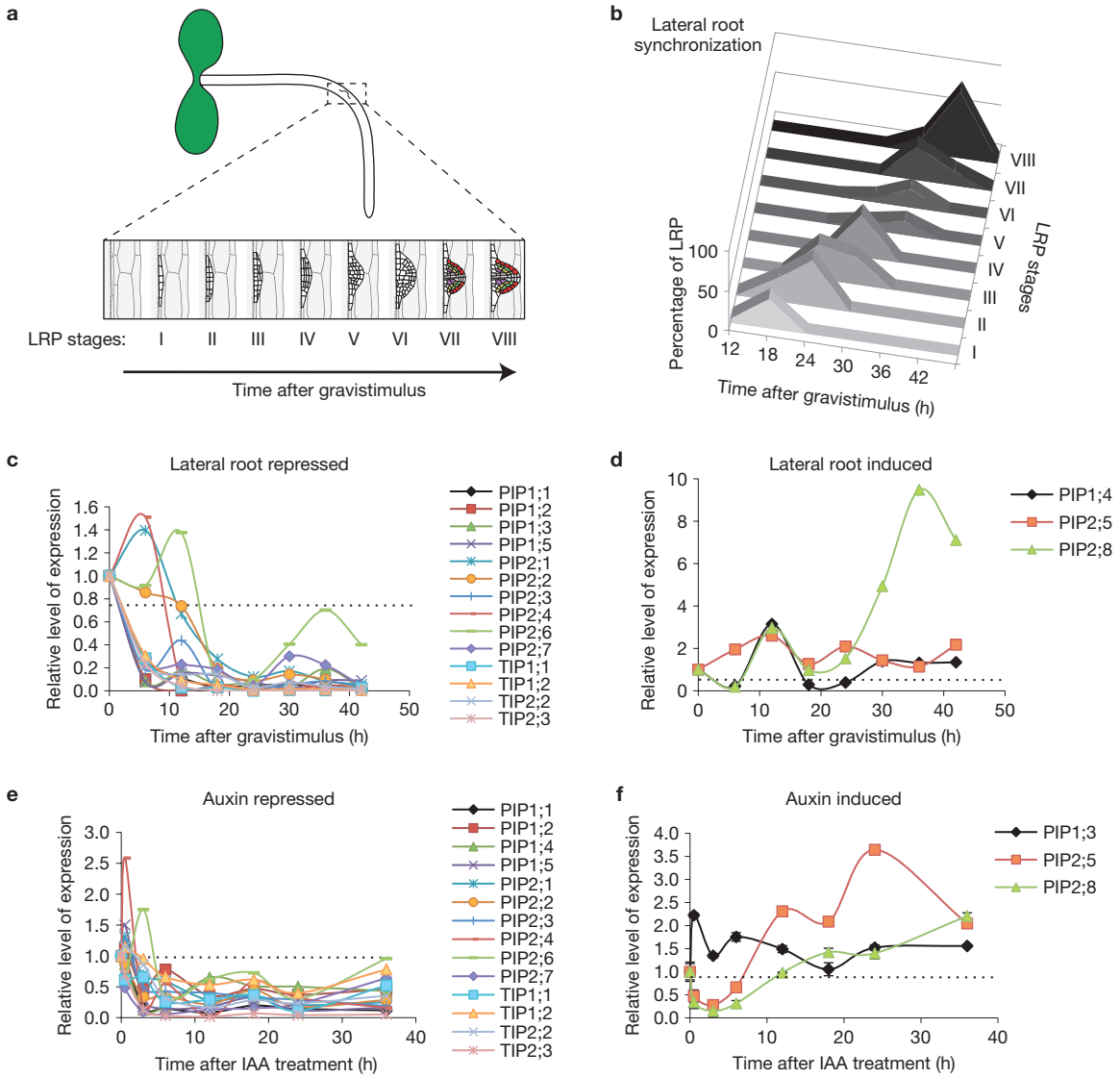

Figure 1 Transcriptional downregulation of aquaporins during lateral root formation is mediated by auxin. (**a**,**b**) Lateral root synchronization was obtained after a 90° gravitropic stimulus. (**a**) An LRP was induced at the root bend created after the stimulus according to previous reports[18]. (**b**) LRP stages (from I to VIII according to previous descriptions[20]) were determined every 6 h post-stimulus and are represented as a percentage of the total number of induced LRP. (**c**,**d**) The aquaporin gene expression level was followed after gravistimulation of lateral root formation and dissection of the root bend. The relative level of expression is shown as a function of time after gravistimulus. (**c**) Out of the 17 major aquaporin genes, 14 genes are repressed during lateral root formation (*PIP1;1, PIP1;2, PIP1;3, PIP1;5, PIP2;1, PIP2;2, PIP2;3, PIP2;4, PIP2;6, PIP2;7, TIP1;1, TIP1;2, TIP2;2* and *TIP2;3*). (**d**) *PIP1;4* and *PIP2;5* show little induction during lateral root formation whereas *PIP2;8* is induced. (**e**,**f**) Auxin generally downregulates aquaporin gene expression. The aquaporin gene expression level was determined in the whole root after treatment with auxin (1 μM IAA) for the indicated time. (**e**) 14 aquaporin genes are repressed by auxin (*PIP1;1, PIP1;2, PIP1;4, PIP1;5, PIP2;1, PIP2;2, PIP2;3, PIP2;4, PIP2;6, PIP2;7, TIP1;1, TIP1;2, TIP2;2* and *TIP2;3*). (**f**) *PIP1;3* and *PIP2;8* show little induction during lateral root formation whereas *PIP2;5* is induced. For clarity, error bars are not included in the graph. Numerical values are provided in Supplementary Table S1.

(Fig. 3b,d). This expression pattern was the exact opposite of the auxin response reporter DR5 (refs 5,21; Fig. 3c), consistent with our results that auxin represses *PIP2;1* expression (Fig. 1e,f). We also observed that auxin treatment resulted in a strong reduction of the *proPIP2;1:GUS* signal (Fig. 3e,f), whereas treatment with the auxin response inhibitor *p*-chlorophenoxy-isobutyric acid (PCIB) resulted in a strong increase of the *proPIP2;1:GUS* signal and extended the spatial pattern into the outer layers (Fig. 3e,g). Our observations suggest that auxin accumulation causes a reduction in *PIP2;1* expression in the LRP.

Expression of *PIP2;8*, which was upregulated at a later phase of lateral root development or after long exogenous auxin treatments (Fig. 1d,f) is largely restricted to the stele (Supplementary Fig. S3a–f). From stage IV onwards, *PIP2;8* expression is induced at the LRP base and underlying stele (Supplementary Fig. S3c–f) but is not altered by exogenous IAA or PCIB treatment (Supplementary Fig. S3g–m). Thus, the auxin-induced enhancement of lateral root number accounts for the apparent auxin-dependent *PIP2;8* upregulation (Supplementary Fig. S3g–i). Taken together, the *PIP2;1* and *PIP2;8* expression data suggest that lateral root development involves a fine

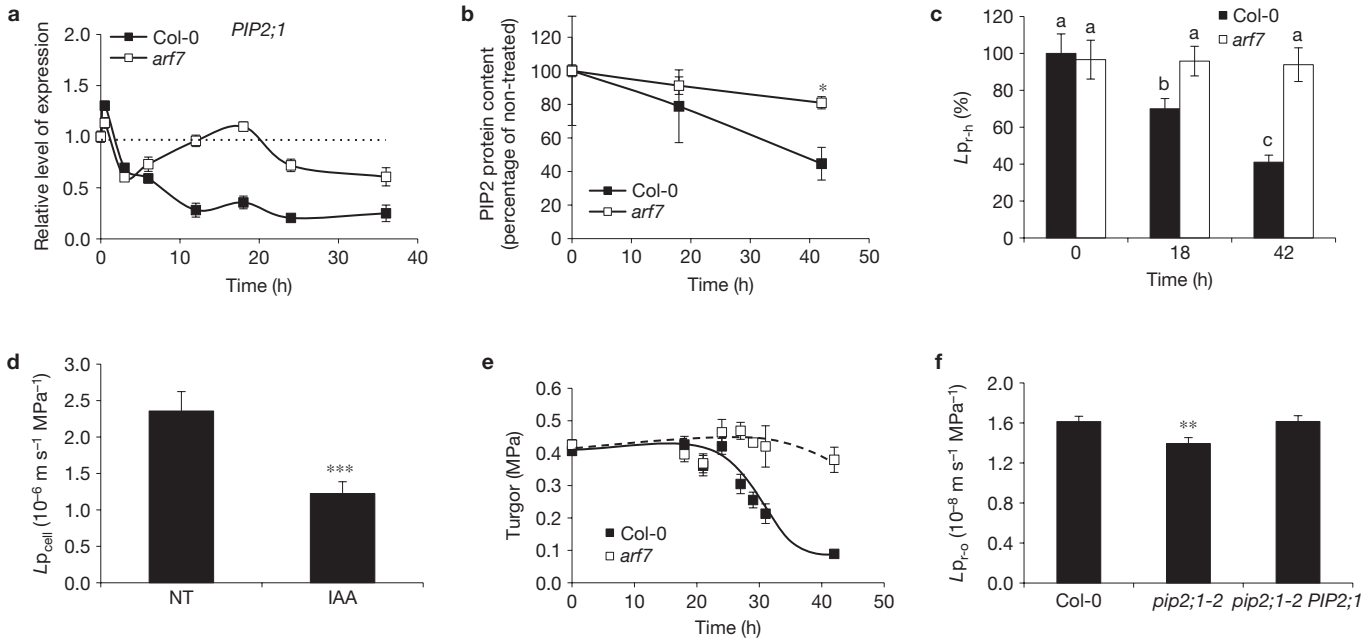

Figure 2 Auxin reduces aquaporin accumulation and hydraulic conductivity. (**a**) Auxin-dependent repression of one of the most highly expressed root isoforms, *PIP2;1*, is *ARF7* dependent. (**b**) The protein content was determined by ELISA with a anti-PIP2 antibody that recognizes PIP2;1, PIP2;2 and PIP2;3. Roots were collected after treatment with 1 μM IAA for the indicated time on wild-type (Col-0) and *arf7* mutant plants. Values are indicated as a percentage of the untreated control from three independent plant cultures. (**c**) Lp_{r-h} was measured after 1 μM IAA treatment for 18 and 42 h on Col-0 and the *arf7* mutant. Values are indicated as a percentage of the untreated Col-0 ($9 < n < 29$). (**d**) Lp_{cell} of Col-0 roots was measured after treatment for 18 h with 1 μM IAA ($n = 22$) and compared with the Lp_{cell} of non-treated (NT) roots. (**e**) Cortical cell turgor was reduced on auxin treatment in Col-0 but not in the *arf7* mutant. (**f**) Lp_{r-o} was determined in the wild type (Col-0), *pip2;1-2* mutant and complemented *pip2;1-2* mutant (*pip2;1-2 PIP2;1*). Data shown are mean value ± s.e.m. with $n = 21$, 18 and 22 assessed from two independent plant cultures. The asterisks indicate a significant difference from the corresponding control experiment by Student's *t*-test ($^{*}P < 0.05$; $^{**}P < 0.01$; $^{***}P < 0.001$). The letters indicate independent groups according to one-way analysis of variance test (**c**).

spatial and temporal control of water exchanges between the stele, LRP and overlaying cells.

Modelling suggests that distinct spatial domains of aquaporin expression are required during LRE

To gain further understanding of the biomechanics of LRE and how this process is affected by the presence of auxin and aquaporins, we developed a mathematical model, which simulates water movement between stele, LRP and overlaying tissues. We considered the tissue scale and modelled the primordium and overlaying tissue as distinct fluid-like compartments, lumping the effects of cell-wall extension and cell-to-cell reorganization into the properties of the boundaries (Fig. 4a).

In the model (see Supplementary Information), we assumed that emergence is driven by increasing osmotic pressure within dividing primordium cells, drawing water into the LRP and resulting in a build-up in turgor pressure. This pressure increases the stress in the LRP boundary, which eventually yields and extends, enabling the LRP to force through the overlaying tissues. The predicted emergence time depends on the material properties of the LRP boundary (characterized by extensibility and yield), initial tissue configuration (considered to be a stage I primordium) and magnitude of water fluxes. The presence of aquaporins increases the boundary permeability whereas auxin accumulation leads to its decrease. Thus, the model enabled us to deduce how LRE is affected by the aquaporin distribution and its regulation by auxin.

The model can be described using differential equations with appropriate initial conditions and kinetic parameters estimated from experiments (see Supplementary Information). We adjusted the rate of increase of the primordium's osmotic pressure so that LRE took 28 h in wild-type plants (Fig. 4b). The model predicted the hydrostatic pressures in the primordium and overlaying tissue, and the direction of the water fluxes through each boundary (shown by arrows in Fig. 4a). The model also revealed how the boundary permeabilities (k_1 to k_4) affect the emergence time (Fig. 4c,d); we obtained a significant influence provided the yield stress of the primordium's boundary is small, suggesting significant cell-wall remodelling as reported previously[5,34]. The model predicted that increasing k_2 or k_4 inhibits emergence by facilitating water movement into overlaying tissues (Fig. 4c,d). In contrast, increasing k_1 promotes emergence by facilitating water inflow into the primordium whereas increasing k_3 has an opposite effect on emergence by favouring water outflow towards the stele (Fig. 4c,d).

Owing to the direction of the water fluxes, the model predicted that, by reducing aquaporin activity in the overlaying tissue (reducing permeability k_2), auxin promotes emergence. However, auxin also inhibits emergence by reducing aquaporin activity in the primordium (reducing permeability k_1). To understand these opposing effects, we removed the influence of auxin from the model (making k_1 and k_2 constant); with appropriate parameter values, we found emergence to be delayed by 8.7 h, indicating that, indeed, auxin has an accelerating effect on LRE. Thus, the model exemplifies how spatial

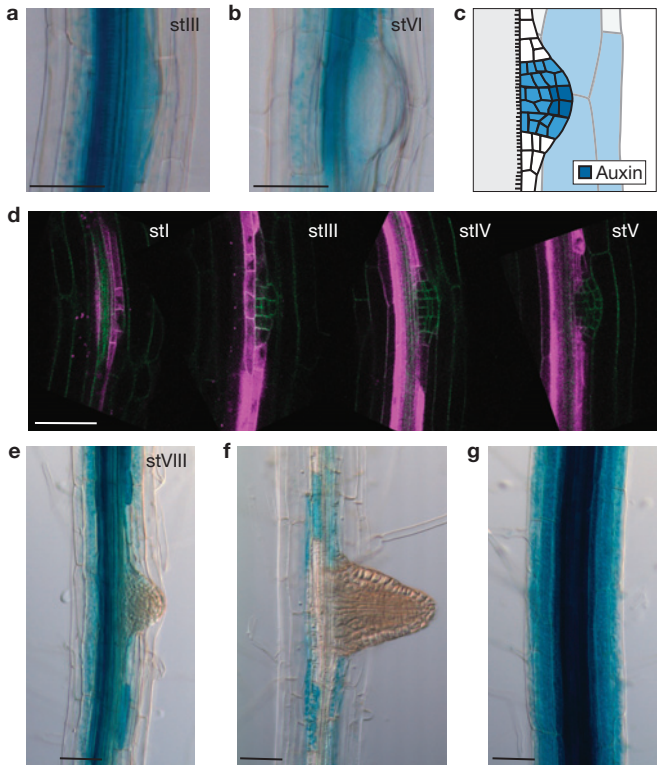

Figure 3 *PIP2;1* expression oppositely mirrors auxin accumulation during lateral root formation. (**a**,**b**) *PIP2;1* expression determined with a transcriptional *proPIP2;1:GUS* fusion. (**c**) Schematic drawing showing auxin accumulation in the LRP and the overlaying tissue as reported by the auxin responsive promoter DR5 (refs 5,21). (**d**) *PIP2;1* expression determined with a translational *proPIP2;1:PIP2;1–mCHERRY* fusion (magenta). Cell shapes are indicated by the plasma-membrane-localized marker (green) encoded by *proUBQ:YFP–NPSN12*. (**e**–**g**) Auxin controls the *PIP2;1* expression pattern: untreated seven-day-old plants (**e**), plants treated with 1 μM IAA for 48 h (**f**) and plants treated with 10 μM PCIB for 24 h (**g**). The lateral root developmental stages are indicated by roman numbers as described previously[20]. Scale bars, 50 μm.

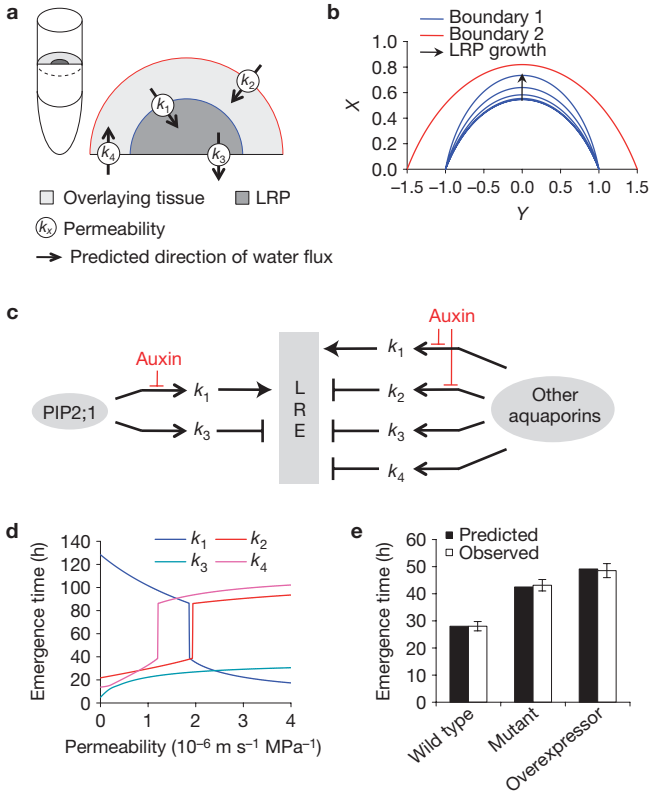

Figure 4 Mathematical model of LRE. (**a**) Two-dimensional tissue-scale model of LRE representing the cross-section of an LRP (dark grey) protruding into the outer tissue (light grey). The arrows show the predicted direction of the water fluxes between compartments; the magnitude of each water flux depends on the boundary's permeability (k_1 to k_4) and the difference in hydrostatic pressure and osmotic potential. (**b**) Simulation of the wild-type LRP emerging through the overlaying tissue. (**c**) Diagram summarizing how auxin and aquaporins affect the permeabilities, and how these in turn affect the predicted emergence time. (**d**) The influence of the permeability values on the predicted emergence time. (**e**) The predicted and observed emergence times in the wild type, the *pip2;1* mutant and the *PIP2;1* overexpressor (see Supplementary Information for choice of parameter values). Data shown are mean value ± s.e.m., and $n = 20$.

and temporal control of auxin-dependent cell hydraulic conductivity could be critical during LRE.

We next used the model to investigate the importance of the cell-specific and dynamic *PIP2;1* distribution. We first simulated LRE with *PIP2;1* expression being ectopic and independent of auxin. This PIP2;1 distribution facilitated water fluxes into the overlaying tissue, resulting in this tissue providing a greater resistance to primordium expansion and therefore delaying LRE by >20 h (Fig. 4e). We then considered a loss-of-function mutant, *pip2;1*, by reducing permeabilities k_1 and k_3 and removing auxin's influence on k_1. Reducing k_1 (inhibiting LRE by reducing fluxes into the primordium) dominates over the influence of reducing k_3 (promoting LRE by reducing fluxes out of the primordium), so that LRE should again occur later than in the wild type (emergence time: 42.5 h), owing to reduced water fluxes from the overlaying tissue to the primordium (Fig. 4e). Thus, the model shows how the spatial distribution of PIP2;1 promotes LRE.

Phenotypes of PIP2;1-knockout and -overexpressing lines validate model predictions

To test model predictions, we studied transgenic lines expressing *PIP2;1* under the control of the strong, constitutive double 35S promoter (*d35S:PIP2;1*). *PIP2;1* overexpression led to a concomitant increase in PIP2 abundance and $Lp_{r\text{-}h}$ (+47 − 63%—Supplementary Fig. S4a,b). In addition, the transgenic lines showed a complete insensitivity of $Lp_{r\text{-}h}$ to auxin inhibition (Supplementary Fig. S4c). Next, wild-type and transgenic roots were given a gravitropic stimulus and LRP were counted and staged at 18 and 42 h pgi (Fig. 5a,b). Wild-type (Col-0) plants accumulated stage I and II LRP 18 h pgi and stage VII and VIII 42 h pgi, respectively (Fig. 5a). Lateral root initiation and first divisions were not affected in *d35S:PIP2;1*, but showed an accumulation of stage II–VIII LRP 42 h pgi (Fig. 5b). This result indicates impaired LRE after aquaporin overexpression, as predicted in the mathematical model (Fig. 4e).

In parallel, we analysed the effects of two independent loss-of-function alleles in *PIP2;1*. Lateral root initiation and first divisions were not affected in the *pip2;1-1* and *pip2;1-2* mutants, but LRE was delayed at 42 h pgi (Fig. 5a,c,d). Mutant *pip2;1-1* and *pip2;1-2* plants transformed with a 4.6-kilobase (kb) genomic fragment containing the full *PIP2;1* gene or a *proPIP2;1:PIP2;1–mCHERRY* construct exhibited a wild-type LRE phenotype on lateral root induction (Fig. 5e,f and

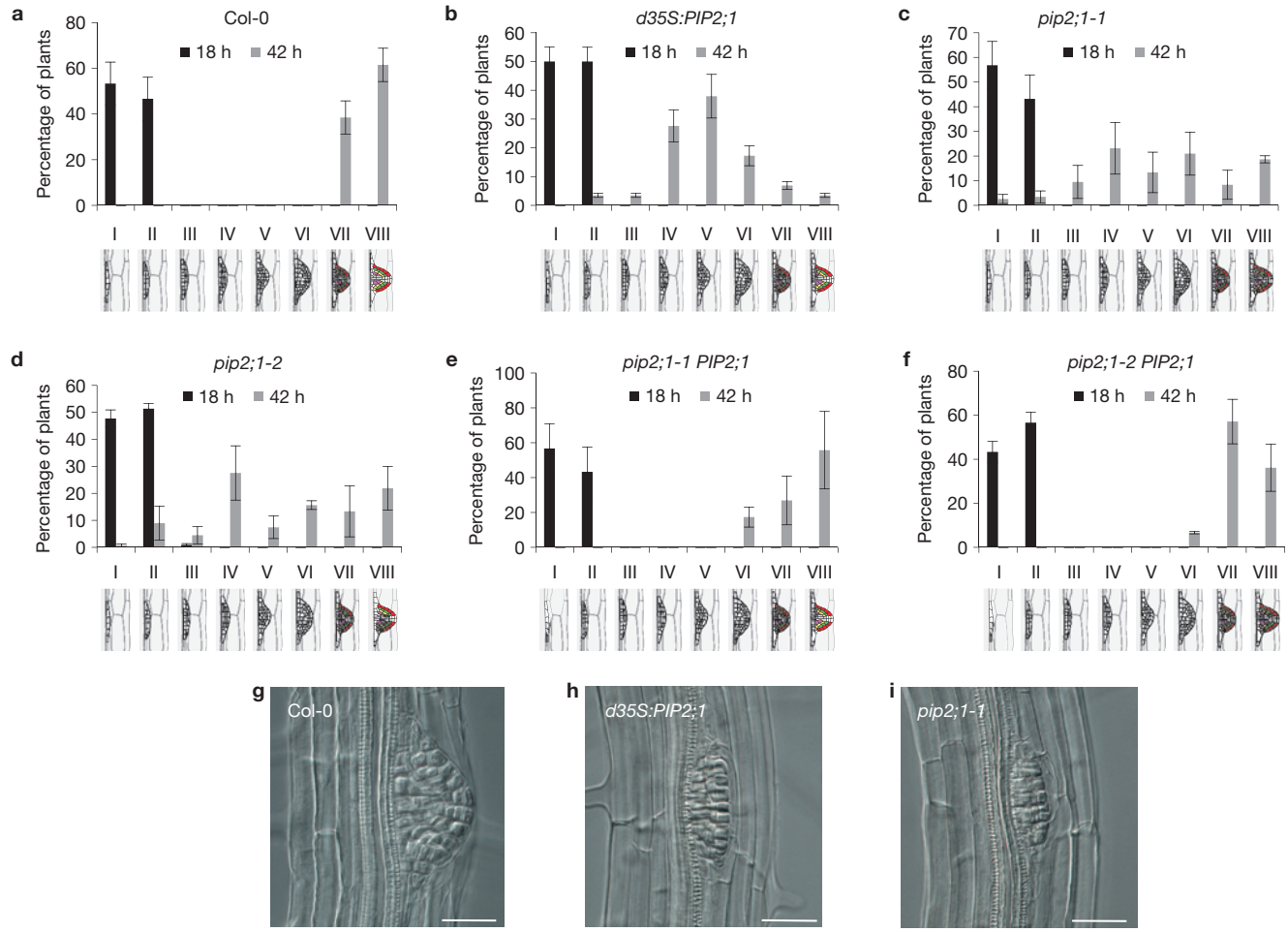

Figure 5 LRE is delayed in the *pip2;1* mutant and the *PIP2;1* overexpressor. (**a**–**f**) LRE phenotyping was achieved by synchronizing lateral root formation with a gravistimulus. Primordia were grouped according to developmental stages as defined previously[20] 18 h pgi (black bars) and 42 h pgi (grey bars). (**a**) Wild-type (Col-0) plants showed accumulation of stage I and II primordium 18 h pgi and accumulation of stage VII and VIII 42 h pgi. (**b**) The *PIP2;1*-overexpression line (*d35S:PIP2;1*) showed similar stages of lateral root formation at 18 h pgi when compared with the wild type, thereby suggesting that early stages of lateral root development were not affected. However, most LRP accumulated at stage IV–VI at 42 h pgi, indicating an emergence defect. (**c**,**d**) LRE is delayed in loss-of-function *pip2;1* mutants. The *pip2;1-1* and *pip2;1-2* mutants showed similar stages of lateral root formation at 18 h pgi when compared to the wild type, thereby suggesting that early stages of lateral root development were not affected. However, only a small amount of LRP reached stages VII and VIII at 42 h pgi in the mutant, indicating an emergence defect. (**e**–**f**) Complementation of both the *pip2;1-1* and *pip2;1-2* mutant alleles with the *PIP2;1* genomic sequence resulted in restoration of the wild-type LRE phenotype. (**g**–**i**) Differential interference contrast imaging at 42 h pgi showed abnormal LRP in the *d35S:PIP2;1* line and the *pip2;1-1* mutant when compared with the dome-shaped wild-type primordium. Data shown are mean value ± s.e.m. and $n = 20$ (**a**–**f**). Scale bars, 25 μm.

Supplementary Fig. S5), demonstrating that the LRE defect was due to disruption of the *PIP2;1* gene. In addition, the LRP shape of both PIP2;1-knockout and overexpressing lines was altered when compared with the wild type (Fig. 5g–i). Whereas wild-type LRP form a dome-shape, mutant LRP were flattened and failed to protrude into overlaying tissues (Fig. 5h,i). Hence, loss of *PIP2;1* function resulted in defective LRE, consistent with the predictions made by the model (Fig. 4e).

DISCUSSION

The hormone auxin represents a key regulator of lateral root development[3]. Previous work has demonstrated that specialized efflux and influx transport proteins cause auxin to accumulate at the apex of new LRP and in overlaying cells, respectively[5,21]. Auxin triggers cell-wall remodelling gene expression in the overlaying cells[34], thereby facilitating primordium emergence through the outer tissues[5]. It was proposed that LRE and concomitant physical modification of the outer tissues must be tightly co-regulated. Here, we demonstrate that auxin also regulates tissue hydraulics to promote LRE.

Auxin regulates root tissue hydraulics by coordinating the repression of aquaporin gene expression in the LRP and overlaying tissues. Application of exogenous auxin and mutant analysis revealed crucial features of hormone action, namely its marked effects on root hydraulics at both the whole-root ($Lp_{r\text{-}o}$ and $Lp_{r\text{-}h}$) and single-cell (Lp_{cell}) levels; dependency on auxin response factor ARF7; and the similar phenotypic defects in LRP shape and LRE kinetics in *arf7* and *pip2;1* mutants (Fig. 5 and Supplementary Fig. S6a–d). These features indicate that regulation of the tissue distribution of aquaporins by auxin fine-tunes the spatial and temporal control of root tissue hydraulics. Although these hydraulic effects can lead to a dynamic decrease in overlaying cells' turgor, as exemplified in the model, turgor measurements in

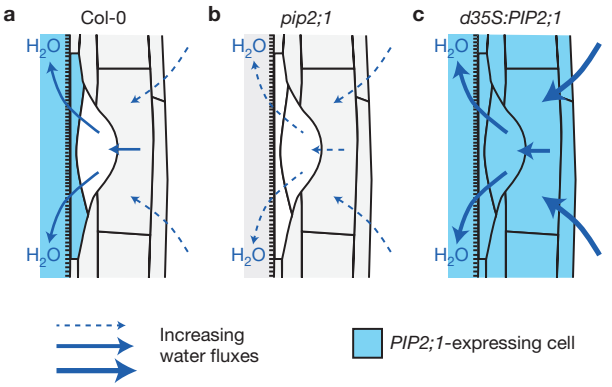

Figure 6 Diagram illustrating the regulation of LRE by PIP2;1. (**a**) Optimal LRE requires water transport into the overlaying tissue to be repressed as a result of auxin accumulation. (**b**) In the *pip2;1* loss-of-function mutant, water transport within the primordium and towards the vasculature is altered, resulting in a reduced LRE rate. (**c**) In the *PIP2;1* gain-of-function mutant, water transport is globally increased, notably in the outer tissue where water transport is normally repressed by auxin. As a result, LRE is delayed.

auxin-treated roots (Fig. 2e) suggested that auxin may also exert more direct effects on steady-state cell turgor. The overall result points to the pivotal role of auxin in controlling the biomechanics of LRE, whereby this hormone affects tissue plasticity (through cell-wall enzymes), water supply (through aquaporins) and turgor maintenance to promote the emergence of developing LRP through overlaying tissues.

Plant roots express numerous aquaporin isoforms[22,23]. The present work focused on the regulation and function of PIP2;1, one of most highly expressed PIPs. Using a high-resolution lateral root synchronization procedure, we showed that disrupting *PIP2;1* gene function impacts lateral root morphogenesis, causing the normal dome-like shape to become flattened, and significantly delays the time taken for the new organ to emerge. *PIP2;1* belongs to a subset of *PIP2* genes (*PIP2;1*, *PIP2;4* and *PIP2;6*) whose messenger RNA abundance exhibits a transient induction before they are repressed along with most other aquaporin genes expressed during lateral root development (Fig. 1c). In only two cases (*PIP2;5* and *PIP2;8*) are *PIP2* transcript levels enhanced throughout lateral root development (Fig. 1d). The spatial pattern of *PIP2;8* expression revealed that it was specifically upregulated at the base of LRP and in the underlying stele (Supplementary Fig. S3). Monitoring the expression patterns and functional importance of every other aquaporin gene family member during lateral root development would provide more insight into their potentially contrasting roles during organ emergence. Preliminary characterization of knockout mutations in other *PIP2* genes has revealed that, similarly to *pip2;1*, they cause a delay in LRE (Supplementary Fig. S6c,e–g). As PIP2;2 is another major root aquaporin with an expression profile similar to PIP2;1 during LRE (Fig. 1c), we also examined the combined loss-of-function mutations in *PIP2;1* and *PIP2;2*. The double mutant showed a delay in LRE similar to the *pip2;1* mutant (Supplementary Fig. S6c,h) consistent with PIP2;1 being the main aquaporin in root tissues. Thus, the present study opens the way to a detailed genetic dissection of the hydraulic control of tissue growth involving other PIP isoforms, at a level of resolution not previously achieved in a plant system.

To probe the tissue-scale regulatory mechanism(s) for how auxin control of aquaporin activity affects LRE, we developed a mathematical model of the root cross-section that describes water fluxes and primordium expansion. Our results suggested that optimal LRE requires water transport into the overlaying tissue to be repressed as a result of auxin accumulation, whereas aquaporins would promote water transfer from the overlaying cells into the primordium (Figs 4a,c and 6a) . These opposing effects on LRE have therefore to be precisely tuned in time and space to explain an overall beneficial effect of auxin and aquaporin activation and repression on LRE. Simulations help provide insight into this integrated process and predict that adding ectopic constitutive *PIP2;1* expression, or removing either tissue-specific *PIP2;1* distribution or auxin inhibition of aquaporins resulted in a reduced emergence rate (Fig. 4), in agreement with experimental observations (Fig. 5). Thus, the model revealed that, in the *pip2;1* loss-of-function mutant, LRE was delayed owing to reduced water transport from the overlaying tissue into the primordium (the k_1 pathway; Fig. 4a and Fig. 6b), whereas in roots of *PIP2;1*-overexpressing plants, it was caused by an increased water supply to the overlaying cells (the k_2 and k_4 pathways; Figs 4a and 6c).

Although the modelling approach allowed us to explain counter-intuitive behaviour, in particular when considering similar LRE phenotypes caused by gain- or loss-of-function of *PIP2*, the phenotypic characterization of additional aquaporin genotypes will help refine this approach and estimates of crucial parameter values. By focusing on the tissue scale, the model also provides a building block in developing future models, which should incorporate the cell scale and three-dimensionality, which we believe will assist in understanding the interplay between the regulation of the water fluxes investigated here, and the remodelling of cell walls, to provide an optimal separation of the overlaying cells. □

METHODS

Methods and any associated references are available in the online version of the paper.

Note: Supplementary Information is available in the online version of the paper

ACKNOWLEDGEMENTS

This work was supported by a Marie Curie Intra-European Fellowship within the 7th European Community Framework Programme PIEF-GA-2008-220506 (B.P.) and by a Grand Federative Project (*Rhizopolis*) of the Agropolis Fondation (Montpellier, France) to C.M. We are indebted to H. Scherb (Helmholtz Zentrum München) for his help with statistical analyses. L.R.B., U.V., M.L., D.M.W., J.R.K., O.E.J. and M.J.B. acknowledge the support of the Biotechnology and Biological Sciences Research Council (BBSRC) and Engineering and Physical Sciences Research Council (EPSRC) funding to the Centre for Plant Integrative Biology (CPIB), BBSRC responsive mode grant support to U.V., L.R.B. and M.J.B. and the BBSRC Professorial Research Fellowship funding to D.M.W. and M.J.B. A.R.S. and O.D.I. acknowledge the support of the Deutsche Forschungsgemeinschaft priority programme SPP1108 (SCHA 454/8).

AUTHOR CONTRIBUTIONS

B.P., G.L., J.Z., U.V., O.P., D-T.L., O.D.I., I.C., M.L., D.M.W., L.L. and P.N. performed experimental work; B.P., G.L., J.Z., L.R.B., J.R.K., O.E.J., A.R.S., C.M. and M.J.B. performed data analysis; B.P., L.R.B., J.R.K., O.E.J., A.R.S., C.M. and M.J.B. oversaw project planning; B.P., L.R.B., A.R.S., C.M. and M.J.B. wrote the paper.

COMPETING FINANCIAL INTERESTS

The authors declare no competing financial interests.

Published online at www.nature.com/doifinder/10.1038/ncb2573
Reprints and permissions information is available online at www.nature.com/reprints

1. Casimiro, I. *et al.* Dissecting *Arabidopsis* lateral root development. *Trends Plant Sci.* **8,** 165–71 (2003).
2. Péret, B., Larrieu, A. & Bennett, M. J. Lateral root emergence: a difficult birth. *J. Exp. Bot.* **60,** 3637–43 (2009).
3. Péret, B. *et al. Arabidopsis* lateral root development: an emerging story. *Trends Plant Sci.* **14,** 399–408 (2009).
4. Overvoorde, P., Fukaki, H. & Beeckman, T. Auxin control of root development. *Cold Spring Harb. Perspect. Biol.* **2,** a001537 (2010).
5. Swarup, K. *et al.* The auxin influx carrier LAX3 promotes lateral root emergence. *Nat. Cell Biol.* **10,** 946–54 (2008).
6. Cosgrove, D. J. Water uptake by growing cells: an assessment of the controlling roles of wall relaxation, solute uptake, and hydraulic conductance. *Int. J. Plant Sci.* **154,** 10–21 (1993).
7. Boyer, J. S. & Silk, W. K. Hydraulics of plant growth. *Funct. Plant Biol.* **31,** 761–773 (2004).
8. Ehlert, C., Maurel, C., Tardieu, F. & Simonneau, T. Aquaporin-mediated reduction in maize root hydraulic conductivity impacts cell turgor and leaf elongation even without changing transpiration. *Plant Physiol.* **150,** 1093–104 (2009).
9. Fricke, W. Biophysical limitation of cell elongation in cereal leaves. *Ann. Bot.* **90,** 157–67 (2002).
10. Hukin, D., Doering-Saad, C., Thomas, C. R. & Pritchard, J. Sensitivity of cell hydraulic conductivity to mercury is coincident with symplasmic isolation and expression of plasmalemma aquaporin genes in growing maize roots. *Planta* **215,** 1047–56 (2002).
11. Oparka, K. J., Prior, D. A. M. & Wright, K. M. Symplastic communication between primary and developing lateral roots of *Arabidopsis thaliana*. *J. Exp. Bot.* **46,** 187–197 (1995).
12. Gomes, D. *et al.* Aquaporins are multifunctional water and solute transporters highly divergent in living organisms. *Biochim. Biophys. Acta* **1788,** 1213–28 (2009).
13. Danielson, J. A. & Johanson, U. Phylogeny of major intrinsic proteins. *Adv. Exp. Med. Biol.* **679,** 19–31 (2010).
14. Kaldenhoff, R. *et al.* Aquaporins and plant water balance. *Plant Cell Environ.* **31,** 658–66 (2008).
15. Maurel, C., Verdoucq, L., Luu, D. T. & Santoni, V. Plant aquaporins: membrane channels with multiple integrated functions. *Annu. Rev. Plant Biol.* **59,** 595–624 (2008).
16. Ditengou, F. A. *et al.* Mechanical induction of lateral root initiation in *Arabidopsis thaliana*. *Proc. Natl Acad. Sci. USA* **105,** 18818–23 (2008).
17. Laskowski, M. *et al.* Root system architecture from coupling cell shape to auxin transport. *PLoS Biol.* **6,** 2721–2735 (2008).
18. Lucas, M., Godin, C., Jay-Allemand, C. & Laplaze, L. Auxin fluxes in the root apex co-regulate gravitropism and lateral root initiation. *J. Exp. Bot.* **59,** 55–66 (2008).
19. Richter, G. L., Monshausen, G. B., Krol, A. & Gilroy, S. Mechanical stimuli modulate lateral root organogenesis. *Plant Physiol.* **151,** 1855–66 (2009).
20. Malamy, J. E. & Benfey, P. N. Organization and cell differentiation in lateral roots of *Arabidopsis thaliana*. *Development* **124,** 33–44 (1997).
21. Benková, E. *et al.* Local, efflux-dependent auxin gradients as a common module for plant organ formation. *Cell* **115,** 591–602 (2003).
22. Alexandersson, E. *et al.* Whole gene family expression and drought stress regulation of aquaporins. *Plant Mol. Biol.* **59,** 469–84 (2005).
23. Monneuse, J. M. *et al.* Towards the profiling of the *Arabidopsis thaliana* plasma membrane transportome by targeted proteomics. *Proteomics* **11,** 1789–97 (2011).
24. Calderon-Villalobos, L. I., Tan, X., Zheng, N. & Estelle, M. Auxin perception–structural insights. *Cold Spring Harb. Perspect. Biol.* **2,** a005546 (2010).
25. Okushima, Y. *et al.* Functional genomic analysis of the AUXIN RESPONSE FACTOR gene family members in *Arabidopsis thaliana*: unique and overlapping functions of ARF7 and ARF19. *Plant Cell* **17,** 444–63 (2005).
26. Okushima, Y., Fukaki, H., Onoda, M., Theologis, A. & Tasaka, M. ARF7 and ARF19 regulate lateral root formation via direct activation of LBD/ASL genes in *Arabidopsis*. *Plant Cell* **19,** 118–30 (2007).
27. Wilmoth, J. C. *et al.* NPH4/ARF7 and ARF19 promote leaf expansion and auxin-induced lateral root formation. *Plant J.* **43,** 118–30 (2005).
28. De Smet, I. *et al.* Bimodular auxin response controls organogenesis in *Arabidopsis*. *Proc. Natl Acad. Sci. USA* **107,** 2705–10 (2010).
29. Santoni, V., Vinh, J., Pflieger, D., Sommerer, N. & Maurel, C. A proteomic study reveals novel insights into the diversity of aquaporin forms expressed in the plasma membrane of plant roots. *Biochem J.* **373,** 289–96 (2003).
30. Javot, H. *et al.* Role of a single aquaporin isoform in root water uptake. *Plant Cell* **15,** 509–22 (2003).
31. Boursiac, Y. *et al.* Stimulus-induced downregulation of root water transport involves reactive oxygen species-activated cell signalling and plasma membrane intrinsic protein internalization. *Plant J.* **56,** 207–18 (2008).
32. Kazama, H. & Katsumi, M. The role of the osmotic potential of the cell in auxin-induced cell elongation. *Plant Cell Physiol.* **19,** 1145 (1978).
33. Da Ines, O. *et al.* Kinetic analyses of plant water relocation using deuterium as tracer-reduced water flux of *Arabidopsis* pip2 aquaporin knockout mutants. *Plant Biol. (Stuttg)* **12** (Suppl. 1), 129–39 (2010).
34. Laskowski, M., Biller, S., Stanley, K., Kajstura, T. & Prusty, R. Expression profiling of auxin-treated *Arabidopsis* roots: toward a molecular analysis of lateral root emergence. *Plant Cell Physiol.* **47,** 788–92 (2006).

METHODS

Growth conditions and plant material. Wild-type Columbia (Col-0), mutants (*arf7-1*[25], *pip2;1* and *pip2;1 pip2;2*) and reporter lines were grown on vertical 1/2 Murashige–Skoog (MS) plates at 23 °C under continuous light (150 μmol m^{-2} s^{-1}). *pip2;1-1* is derived from the AMAZE collection[35] and the En-transposon is inserted after the 69th nucleotide of the second exon; *pip2;1-2*, *pip2;2-3* and *pip2;2-4* have been described previously[33]. *pip2;4-1* (SM_3_20853; ref. 36) and *pip2;6-3* (SALK_ 092140; ref. 37) were obtained from the Nottingham Arabidopsis Stock Centre[38] and verified by genotyping and RT–PCR. The *pip2;1 pip2;2* double mutant was generated by crossing *pip2;1-2* and *pip2;2-3*. *proPIP2;1:GUS* lines have been described previously[33]. A fragment comprising 2,526 base pairs upstream of the start codon of *PIP2;8* (At2g16850) was cloned into pBGWFS7 to generate transcriptional *proPIP2;8:GUS* fusions. For lateral root phenotypical analysis, lateral root induction was performed on three-day-old seedlings by rotating the plates at 90°. For expression analysis, six-day-old plants were transferred on vertical 1/2 MS plates supplemented with 1 μM IAA or 10 μM PCIB for the indicated time. For root water transport measurements and ELISA assays, plants were germinated and grown on plates for 10 days before transfer to hydroponic culture, as previously described[30]. Plants were further grown for 10–20 days, in a growth chamber at 70% relative humidity with cycles of 16 h of light (250 μmol m^{-2} s^{-1}) at 22 °C and 8 h of dark at 21 °C.

Nucleic-acid manipulations and constructs. For overexpression of *A. thaliana* PIP2;1, the complementary DNA of PIP2;1 was placed under the control of a double enhanced CaMV 35S promoter and transferred into plants through *Agrobacterium* by floral dipping[39] using a pGreen179 binary transformation vector. Three plant lines that showed the highest expression of the transgene were selected among 200 transformed lines by western blot analyses on leaf extract using an anti-PIP2 antibody[29] (see below). Plants co-expressing the *PIP2;1–mCHERRY* construct under the control of 1.5 kb of genomic sequences upstream of the *PIP2;1* start codon, and the *YFP–AtNPSN12* construct under the control of a promoter of ubiquitin 10 gene[40] were obtained by crossing the plants that individually express the constructs. *At* NPSN12 is a SNARE protein, which has been localized in the plasma membrane[40].

Mutant complementation. A 4.6 kb genomic *PIP2;1* fragment was amplified by PCR using primers 5′-ATTTGTCCTTTCCGGTACAAT-3′ (forward) and 5′-ACTCTCAATCCTCAGCCAAGT-3′ (reverse) and cloned into pDONR221 vector, verified by sequencing and subsequently cloned into pBGW and transformed by floral dipping[39] into the two *pip2;1* mutant alleles. Homozygous, complemented plants with single insertion were confirmed on the basis of antibiotic (phosphinotricine) resistance and further confirmed by RT–PCR.

qRT–PCR. Total RNA was extracted from roots using a Qiagen RNeasy plant mini kit with on-column DNAse treatment (RNAse free DNAse set, Qiagen). Poly(dT) cDNA was prepared from 2 μg total RNA using the Transcriptor first-strand cDNA synthesis kit (Roche). qPCR was performed using SYBR Green Sensimix (Quantace) on Roche LightCycler 480 apparatus. PCR was carried out in 384-well optical reaction plates heated for 1 min to 95 °C, followed by 40 cycles of denaturation for 5 s at 95 °C, annealing for 8 s at 62 °C and extension for 30 s at 72 °C. Target quantifications were performed with the specific primer pairs described in Supplementary Fig. S7. Expression levels were normalized to the ubiquitin-associated gene *UBA* (At1g04850) using the following primers *UBA* forward 5′-agtggagaggctgcagaaga-3′ and *UBA* reverse 5′-ctcgggtagcacgagcttta-3′. All qRT–PCR experiments were performed in triplicate and the values represent means ± s.e.m.

Hydraulic conductivity measurement. Measurements of root hydrostatic hydraulic conductivity (Lp_{r-h}) and root osmotic hydraulic conductivity (Lp_{r-o}) were performed as described previously[30,41]. Pressure probe measurements in root cortical cells and calculation of cell hydraulic conductivity were made as previously described[30].

Immunodetections. Serial twofold dilutions in a carbonate buffer (30 mM Na_2CO_3, 60 mM $NaHCO_3$, at pH 9.5) of 0.5 μg of membrane extracts were loaded in triplicate on immunoplates (Maxisorp). The ELISA assay was performed as previously described[42] using a 1:2,000 dilution of an anti-PIP2 antibody raised against a 17-amino-acid carboxy-terminal peptide of *At* PIP2;1 (ref. 29). Western blot analysis was performed using classical procedures[29] and the same anti-PIP2 antibody.

Histochemical analysis and microscopy. GUS staining was done as previously described[43]. Plants were cleared for 24 h in 1 M chloral hydrate and 33% glycerol. Seedlings were mounted in 50% glycerol and observed with a Leica DMRB microscope. For confocal microscopy, images were captured with an inverted confocal laser-scanning microscope (Inverse 1 Axiovert 200M Zeiss/LSM 510 META Confocal) with a 63× oil-immersion objective. The emitted fluorescence signal was captured by alternately switching the 488 nm and 543 nm excitation lines. Lateral roots were imaged as 1 μm step *z* series.

Mathematical modelling. Full details of the model formulation and predictions are provided in the Supplementary Information. Details of the modelling are available in Supplementary Note S1 and Matlab code is available in Supplementary Data S1. Simulations were performed in Matlab and the numerical code can be downloaded from www.cpib.ac.uk/tools-resources/models.

35. Wisman, E., Cardon, G. H., Fransz, P. & Saedler, H. The behaviour of the autonomous maize transposable element En/Spm in *Arabidopsis thaliana* allows efficient mutagenesis. *Plant Mol. Biol.* **37,** 989–99 (1998).
36. Tissier, A. F. *et al.* Multiple independent defective suppressor-mutator transposon insertions in *Arabidopsis*: a tool for functional genomics. *Plant Cell* **11,** 1841–52 (1999).
37. Alonso, J. M. *et al.* Genome-wide insertional mutagenesis of *Arabidopsis thaliana*. *Science* **301,** 653–657 (2003).
38. Scholl, R. L., May, S. T. & Ware, D. H. Seed and molecular resources for *Arabidopsis*. *Plant Physiol.* **124,** 1477–1480 (2000).
39. Clough, S. J. & Bent, A. F. Floral dip: a simplified method for Agrobacterium-mediated transformation of *Arabidopsis thaliana*. *Plant J.* **16,** 735–43 (1998).
40. Geldner, N. *et al.* Rapid, combinatorial analysis of membrane compartments in intact plants with a multicolor marker set. *Plant J.* **59,** 169–78 (2009).
41. Postaire, O. *et al.* A PIP1 aquaporin contributes to hydrostatic pressure-induced water transport in both the root and rosette of *Arabidopsis*. *Plant Physiol.* **152,** 1418–30 (2010).
42. Boursiac, Y. *et al.* Early effects of salinity on water transport in *Arabidopsis* roots. Molecular and cellular features of aquaporin expression. *Plant Physiol.* **139,** 790–805 (2005).
43. Péret, B. *et al.* Auxin influx activity is associated with Frankia infection during actinorhizal nodule formation in *Casuarina glauca*. *Plant Physiol.* **144,** 1852–62 (2007).

nature cell biology

DOI: 10.1038/ncb2573

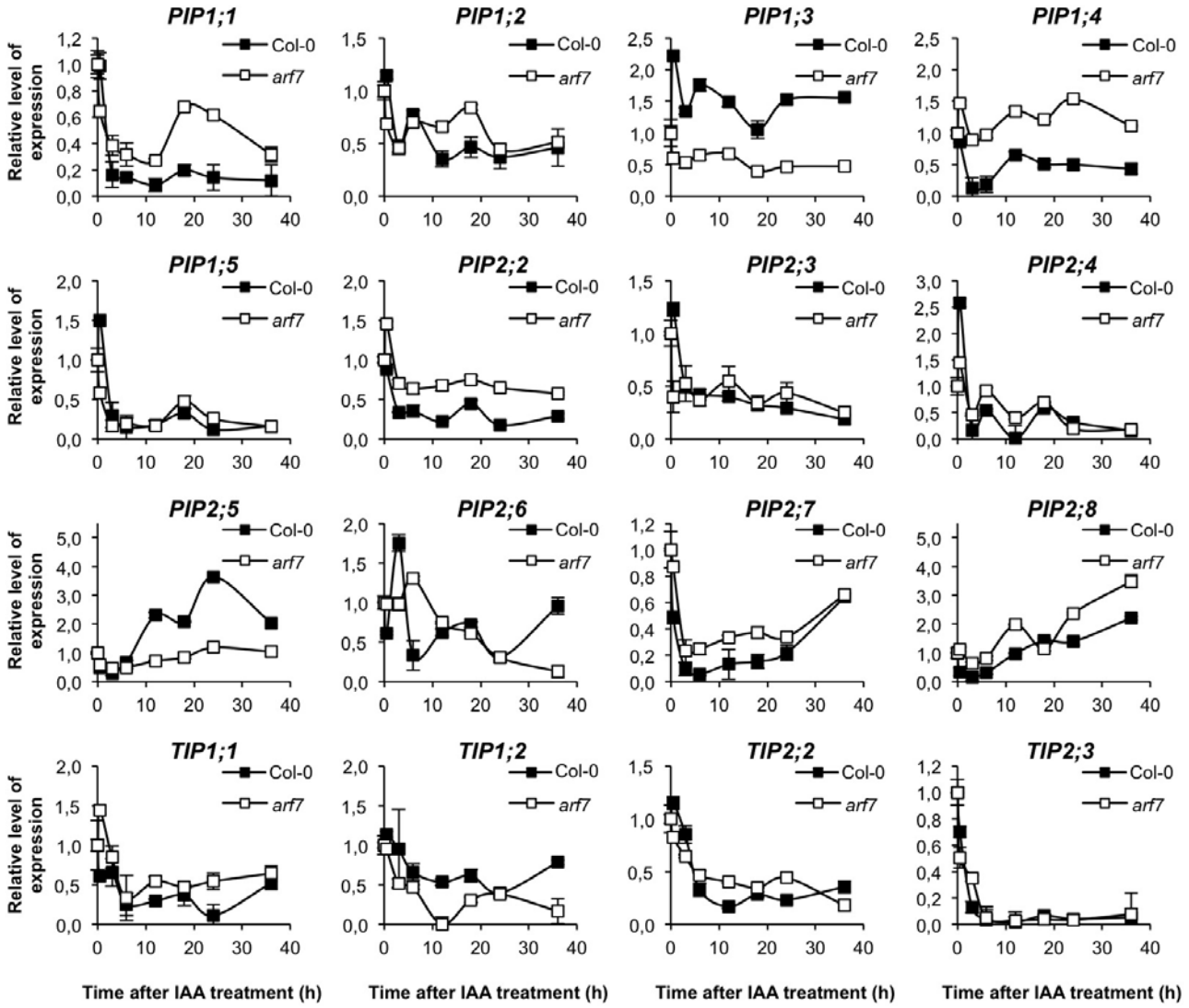

Figure S1 Expression analysis of the major aquaporin genes. Average relative level of expression and sem values of aquaporin genes (*PIP1;1, PIP1;2, PIP1;3, PIP1;4, PIP1;5, PIP2;2, PIP2;3, PIP2;4, PIP2;6, PIP2;7, TIP1;1, TIP1;2, TIP2;2,* and *TIP2;3*) upon 1 μM IAA treatment in the wild type (WT) and *arf7* mutant backgrounds. Time is indicated in hours.

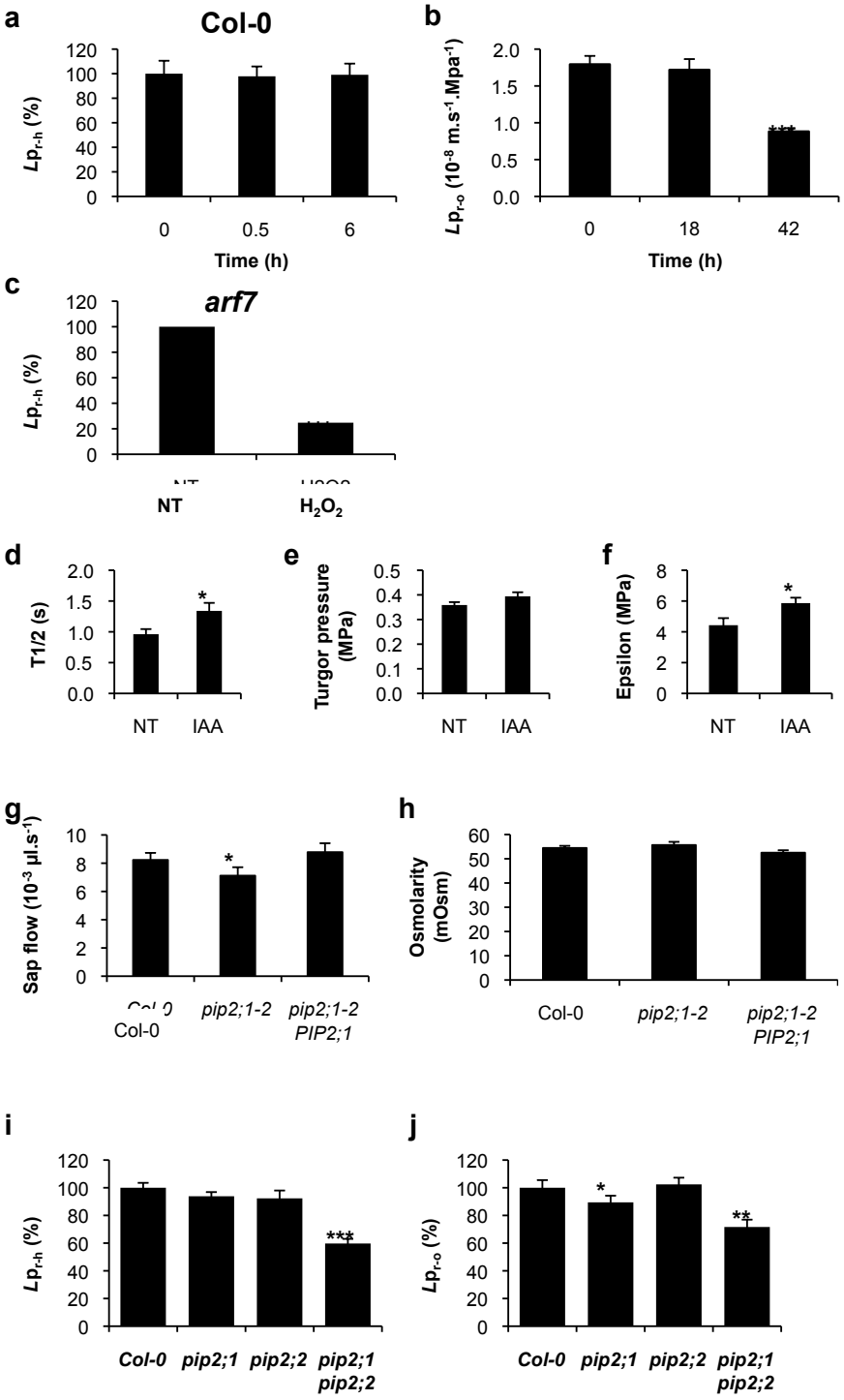

Figure S2 Supplementary root hydraulic conductivity measurements. (**a**) Short time 1 µM IAA treatment did not affect hydrostatic root hydraulic conductivity ($Lp_{r\text{-}h}$) of the wild-type (Col-0) plants (n = 5). (**b**) $Lp_{r\text{-}o}$ of Col-0 roots treated with 1 µM IAA for 18 h and 42 h was determined. Data shown are mean value ± sem with n =14, 14, 15 from 2 independent plant cultures..(**c**) The *arf7* mutant $Lp_{r\text{-}h}$ is strongly affected by a H_2O_2 treatment (5 mM for 20 min) The mean of 2 experiments is shown.(NT, non-treated roots (**d-f**) Water relation parameters were determined in single root cortical cells of non-treated plants (NT) or plants treated with 1 µM IAA for 18 hours (IAA). Cell hydraulic conductivity was calculated from the half-time of water exchange ($T_{1/2}$) (d), the stationary turgor pressure (e) and the volumetric elastic modulus (Epsilon) (f) (n = 22) (**g-h**) Characterization of free sap exudation in roots from wild type (Col-0) and *pip1;2-2* mutant plants complemented (*pip2;1-2* PIP2;1) or not (*pip2;1-2*) with a *PIP2;1* genomic fragment. Sap flow rate (g) and osmolarity (h) was used to deduce the $Lp_{r\text{-}h}$ $Lp_{r\text{-}o}$ values shown in Fig. 2f. Data shown are mean value ± sem from 2 independent plant cultures (n=21, 18, 22). (**i, j**) $Lp_{r\text{-}h}$ (i), data shown are mean value ± sem with n =35, 13, 18 from 2 independent plant cultures and $Lp_{r\text{-}o}$ (j), data shown are mean value ± sem with n =27, 21, 14 from 3 independent plant cultures, of Col-0 and single or double knock-outs for *PIP2;1* (*pip2;1*) and *PIP2;2* (*pip2;2*). Asterisks indicate a significant difference with corresponding control experiment by Student's t-test (*: $p < 0.05$; **: $p < 0.01$; ***: $p < 0.001$).

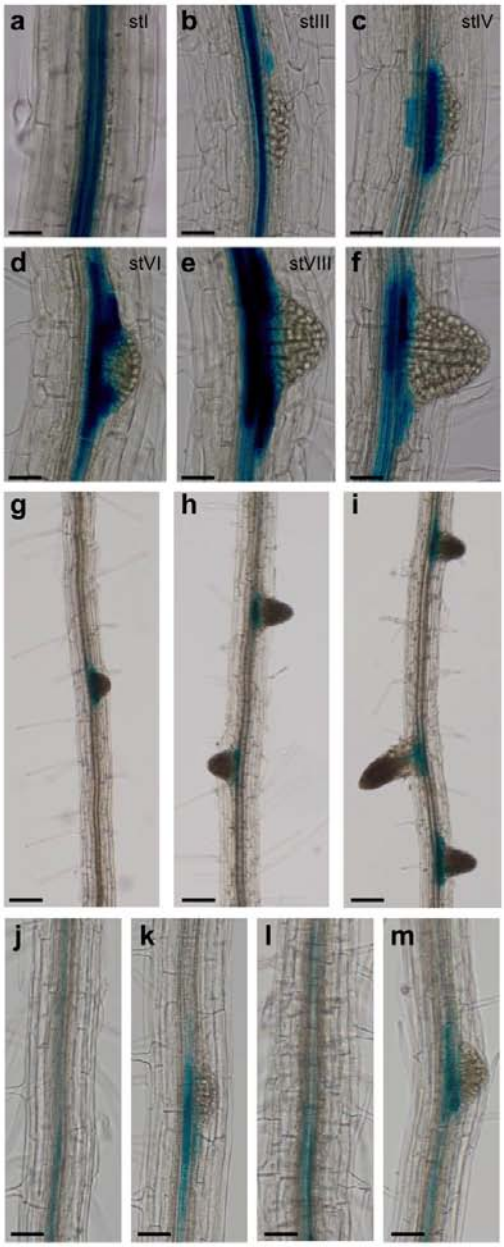

Figure S3 Characterization of the *PIP2;8::GUS* reporter lines. (**a-f**) *PIP2;8* expression determined with a transcriptional *proPIP2;8:GUS* fusion during lateral root development. LR developmental stages are indicated by Roman numbers as described previsouly[20]. Expression pattern was verified with three independent transgenic lines. (**g-m**) Auxin and anti-auxin treatments did not affect *proPIP2;8:GUS* expression pattern. Untreated 7 day-old plants (g, j, k), plants treated with 1 µM IAA for 48 hours (h,i) and plants treated with 10 µM PCIB for 24 hours (l,m). The results were verified using an independent transgenic line. Scale bars represent 50 µm (a-f), 75 µm (j-m) and 100 µm (g-i).

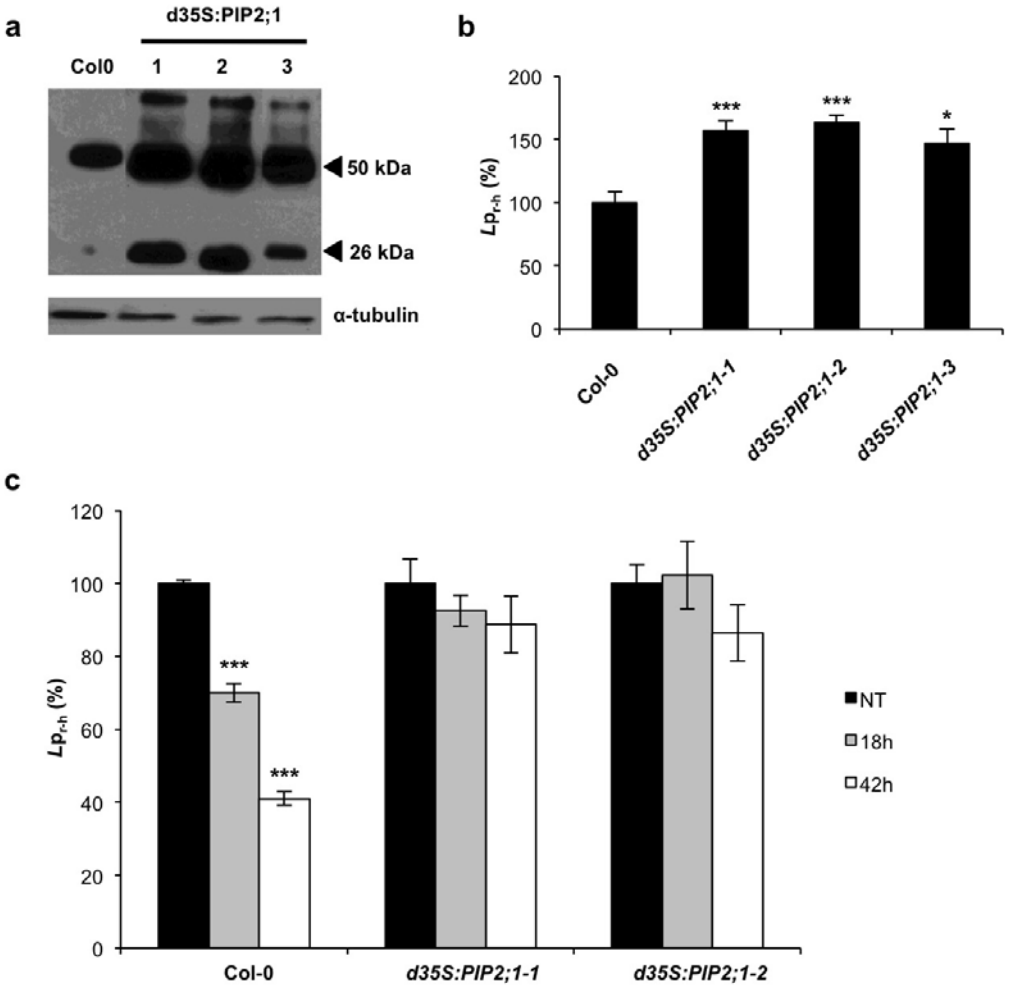

Figure S4 Characterization of the *PIP2;1* over-expression lines. (**a**) Western blot of three independent *d35S:PIP2;1* lines (lanes 1 to 3) showing strong accumulation of the PIP2 proteins compared to wild type (Col-0). The two bands correspond to monomeric and dimeric forms. Representative experiment with 5 µg proteins per lane. ELISA assays on the same samples showed that, with respect to Col-0, proteins immunoreactive to the anti-PIP2 antibody were increased by 2.6-2.9-fold in the *d35S:PIP2;1* lines (**b**) Hydrostatic root hydraulic conductivity (Lp_{r-h}) is increased in three independent *d35S:PIP2;1* lines (1 to 3). Data shown are mean value ± sem with n =21, 20, 17, 16 from 3 independent plant cultures (**c**) The reduction of root hydraulic conductivity by auxin is suppressed in the *PIP2;1* over-expression lines. Lp_{r-h} was determined upon 18 and 42 hours treatments with 1 µM IAA and indicated as a percentage of untreated control. Data shown are mean value ± sem with n =21, 13, 19, 9, 8, 12, 7, 6, 10 from 2 independent plant cultures. Asterisks indicate a significant difference with corresponding control experiment by Student's t-test (*: $p < 0.05$; ***: $p < 0.001$).

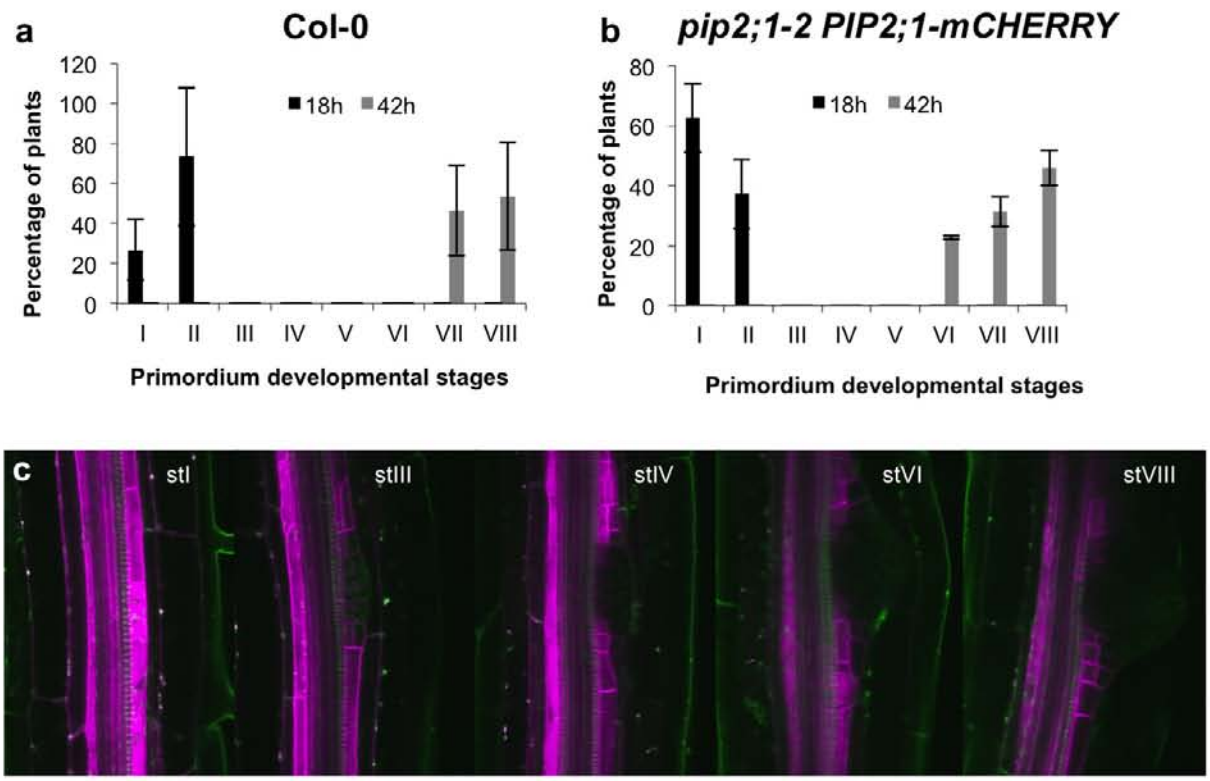

Figure S5 The PIP2;1-mCHERRY fusion rescues the *pip2;1* LR emergence phenotype. (**a-b**) Expressing the *proPIP2;1:PIP2;1-mCHERRY* construct in the *pip2;1-2* mutant background (b) restores kinetics of LR emergence similar to those in wild-type (Col-0, a). (**c**) Expression pattern driven by the *proPIP2;1:PIP2;1-mCHERRY* construct in the *pip2;1-2* background is similar to the expression driven when expressing the same construct in the wild-type (Col-0) background (as shown in Figure 3d).

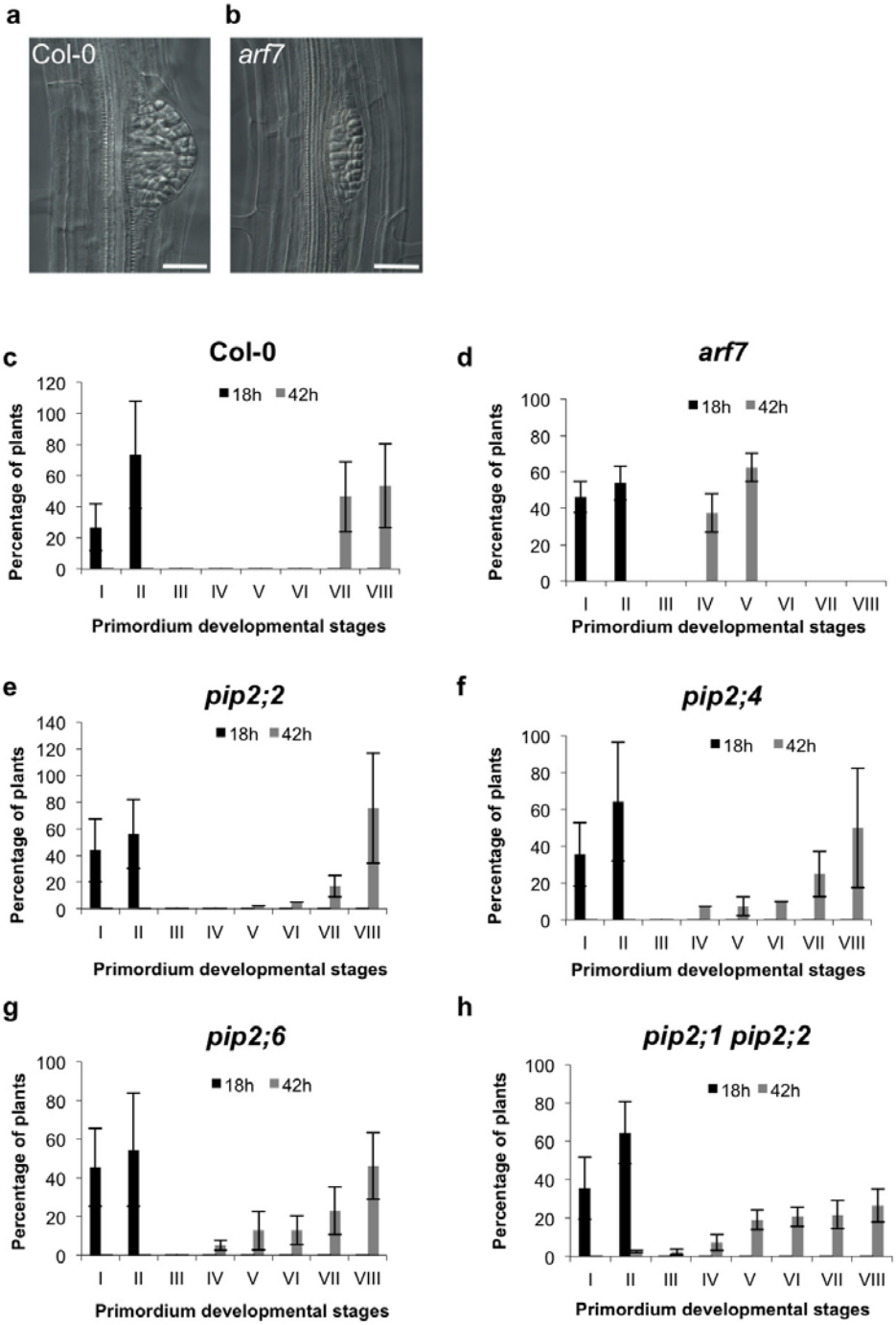

Figure S6 Lateral root emergence is defective in *arf7* mutants and in single or multiple *pip2* mutants. LRE phenotyping was achieved by synchronizing LR formation with a gravistimulus (**a,b**) Differential interference contrast imaging at 42 hours post-induction (hpi) showed abnormal LR primordia of *arf7* mutants (b) compared to dome-shaped wild-type primordium (a). Scale bars represent 25 µm (**c-h**) Primordia were grouped according to developmental stages as previously defined[20] 18 hpi (black bars) and 42 hpi (grey bars). (**c**) Wild-type (Col-0) plants showed accumulation of stage I and II primordium 18 hpi and accumulation of stage VII and VIII 42 hpi. (**d**) *arf7* mutants showed similar stages of LR formation at 18 hpi compared to wild type thereby suggesting that early stages of LR development were not affected. However, most LRP accumulated at stage IV and V 42 hpi indicating a strong emergence defect. (**c-e**) The *pip2;2, pip2;4 and pip2;6* single mutants and the double *pip2;1 pip2;2* mutant showed similar stages of LR formation at 18 hpi compared to wild type thereby suggesting that early stages of LR development were not affected. However, they present an accumulation of stages IV to VI LR primordia at 42 hpi indicating an emergence defect. The double *pip2;1 pip2;2* mutant (h) also showed a reduced amount of LRP reaching stage VIII at 42 hpi Data shown are mean value ± sem and n = 20 (c-h).

AGI	Primer name	Primer sequence
At3g61430	qPIP1;1F	CTGGCCTTGTCCTTAGTTGCTTC
	qPIP1;1R	TCTCCTTTGGAACTTCTTCCTTG
At2g45960	qPIP1;2F	TCCTCTTCTTTGCCTAATGGAGAC
	qPIP1;2R	AGTTGCCTGCTTGAGATAAAC
At1g01620	qPIP1;3F	GCTGTGGATGATCTGGTTTTATCG
	qPIP1;3R	GCCGAAACAATATGGATCTTACTC
At4g00430	qPIP1;4F	CTCTGAAGTCTAAGGTGATTAGTGC
	qPIP1;4R	CAACCCGAGAACTTGATGTTGA
At4g23400	qPIP1;5F	TGTTTCCTATGTCATGTGTGATG
	qPIP1;5R	GTACACAATGTATTCTTCCATTGAC
At3g53420	qPIP2;1F	TGTGTTTTCCACTTGCTCTTTTG
	qPIP2;1R	CACAACGCATAAGAACCTCTTTGA
At2g37170	qPIP2;2F	GGCAACTTTGCTTGTAAAACTATGC
	qPIP2;2R	AGTACACAAACATTGGCATTGG
At2g37180	qPIP2;3F	GAAACATATCCTCTTTTCCACTCG
	qPIP2;3R	CTCAATACACCAAACTTACATACG
At5g60660	qPIP2;4F	CTCCTTTAGGAGCTTTGCTTAAT
	qPIP2;4R	CCACATTTACAATTACACGAATGG
At3g54820	qPIP2;5F	GATATGCTCTTCCCTGAGTACATC
	qPIP2;5R	AATATCTCTCCTCACCAAAGCTAG
At2g39010	qPIP2;6F	TTTCGAACTAGCGAAGAGGTGAAG
	qPIP2;6R	AGACACAGTAAATGTCACTCACC
At4g35100	qPIP2;7F	TGTGTAATGAGAGAGATGGTGGA
	qPIP2;7R	AGAGAAACCAAAGGCAAACGA
At2g16850	qPIP2;8F	CAACCCAACCAATTGATGATTCA
	qPIP2;8R	ACATGAAAGAAAGCAACGGAC
At2g36830	qTIP1;1F	CTCCCAACCACAGACTACTGAA
	qTIP1;1R	GCACGATCATAAACCCCTTG
At3g26520	qTIP1;2F	GCATCGTAATGGGTTTCTGG
	qTIP1;2R	TACAATTGCACAAAAGCCTTCC
At4g17340	qTIP2;2F	AGCTCCCACCACAGAAAGCTA
	qTIP2;2R	TTTGGAAGAAACGAGGACCA
At5g47450	qTIP2;3F	GTGAGATCCGAGTGTAATTGACTG
	qTIP2;3R	TTTTCTTTTCTCTACATACAATCTTGC

Figure S7 List of primers used for quantitative RT-PCR. Primer sequences are given from 5' to 3'.